Nitric Oxide–dependent Activation of p53 Suppresses Bleomycin-induced Apoptosis in the Lung

By Darren W. Davis,*‡ Douglas A. Weidner,§ Andrij Holian,*‖ and David J. McConkey*‡

*From the *Program in Toxicology, University of Texas-Houston Graduate School of Biomedical Sciences, Houston, Texas 77030; the ‡Department of Cancer Biology and the §Department of Molecular Hematology and Therapy, University of Texas-MD Anderson Cancer Center, Houston, Texas 77030; and the ‖Department of Pulmonary and Critical Care Medicine, University of Texas Medical School, Houston, Texas 77030*

Abstract

Chronic inflammation leading to pulmonary fibrosis develops in response to environmental pollutants, radiotherapy, or certain cancer chemotherapeutic agents. We speculated that lung injury might be mediated by p53, a proapoptotic transcription factor widely implicated in the response of cells to DNA damage. Intratracheal administration of bleomycin led to caspase-mediated DNA fragmentation characteristic of apoptosis. The effects of bleomycin were associated with translocation of p53 from the cytosol to the nucleus only in alveolar macrophages that had been exposed to the drug in vivo, suggesting that the lung microenvironment regulated p53 activation. Experiments with a thiol antioxidant (*N*-acetylcysteine) in vivo and nitric oxide (NO) donors in vitro confirmed that reactive oxygen species were required for p53 activation. A specific role for NO was demonstrated in experiments with inducible nitric oxide synthase (iNOS)$^{-/-}$ macrophages, which failed to demonstrate nuclear p53 localization after in vivo bleomycin exposure. Strikingly, rates of bleomycin-induced apoptosis were at least twofold higher in p53$^{-/-}$ C57BL/6 mice compared with heterozygous or wild-type littermates. Similarly, levels of apoptosis were also twofold higher in the lungs of iNOS$^{-/-}$ mice than were observed in wild-type controls. Consistent with a role for apoptosis in chronic lung injury, levels of bleomycin-induced inflammation were substantially higher in iNOS$^{-/-}$ and p53$^{-/-}$ mice compared with wild-type controls. Together, our results demonstrate that iNOS and p53 mediate a novel apoptosis-suppressing pathway in the lung.

Key words: NOS-2 • TUNEL • macrophage • oxygen radical • inflammation

Introduction

Pulmonary toxicity leading to epithelial hyperplasia, inflammation, and fibrosis is the unfortunate consequence of exposure of the lung to environmental contaminants, γ irradiation, and a variety of cancer chemotherapeutic agents (1, 2). Early administration of corticosteroids can alleviate (but not prevent) inflammation associated with these responses, but there is no effective treatment for pulmonary fibrosis, and mortality in these patients is high (~50% within 5 yr; reference 2). Furthermore, a relationship between dose and risk of developing lung injury appears to exist in most cases, but this association is poorly understood, and it is currently impossible to predict which patients will develop lung disease. Risk factors include age, simultaneous or prior therapy with other agents, and hyperbaric oxygen therapy (3), but disease onset can occur many years after exposure for reasons that are still not clear. Overall, very little is known about the pathophysiological event(s) underlying the initiation of pulmonary fibrosis.

One feature shared by all of the fibrogenic agents discussed above is their capacity to induce DNA damage in target cells. Genotoxic damage initiates a cellular response involving the tumor suppressor, p53, which acts to inhibit cell cycle progression and activate DNA repair (4, 5) and/or to stimulate apoptosis (6). Reactive oxygen species appear to play a critical role in regulating p53 function (7), and p53 controls the expression of a large number of redox regulatory proteins (8). In particular, recent work has

Address correspondence to David J. McConkey, Department of Cancer Biology-173, U.T. M.D. Anderson Cancer Center, 1515 Holcombe Blvd., Houston, TX 77030. Phone: 713-792-8591; Fax: 713-792-8747; E-mail: dmcconke@notes.mdacc.tmc.edu

shown that nitric oxide (NO) controls p53 activation, and that p53 can regulate inducible NO synthase (iNOS)[1]/NOS-2 promoter activity (9). Given the unique role of oxygen in the lung microenvironment (10), it is likely that p53 plays a critical role in the maintenance of normal lung physiology. The frequent detection of signature inactivating p53 mutations in lung cancer indicates that disruption of the pathway contributes to neoplastic transformation (11, 12).

One of the features of apoptosis that distinguishes the process from necrosis is the lack of associated inflammation. However, apoptotic cells in tissues are usually cleared very rapidly, and the potential consequences of defective clearance are not known. Antibodies to apoptosis-associated antigens (DNA, poly[ADP-ribose] polymerase, phosphatidylserine, DNA-dependent protein kinase) are commonly detected in patients with autoimmune disease (13), and Savill et al. (14) have speculated that apoptosis plays an important role in inflammatory injury to the kidney (glomerulonephritis). Given that uptake of apoptotic bodies serves as one source of antigens for presentation by dendritic cells (15), it is possible that chronic exposure to apoptotic debris is involved in inflammatory lung injury. As a first step in testing this hypothesis, the biological mechanism(s) mediating apoptosis and cellular targets must be identified. Considering the evidence outlined above, we speculated that iNOS and/or p53 might be required for apoptosis induction and subsequent inflammation. To test this possibility directly, we analyzed the effects of one widely studied stimulus for pulmonary fibrosis, the cancer chemotherapeutic agent bleomycin, on p53 activity and apoptosis in wild-type, iNOS$^{-/-}$, and p53$^{-/-}$ C57BL/6 mice, because this strain is considered fibrosis prone (16).

Materials and Methods

Mice. iNOS knockout (iNOS$^{-/-}$) mice (17) were provided by Dr. Carl Nathan (Cornell University, New York, NY). Heterozygous (p53$^{+/-}$) C57BL/6 breeding pairs were obtained from The Jackson Laboratory. Animals were bred and housed in a specific pathogen-free animal facility of the Department of Cancer Biology at the University of Texas M.D. Anderson Cancer Center. Mice were genotyped by PCR amplification of tail DNA according to a protocol that was provided by Dr. Tyler Jacks (Massachusetts Institute of Technology, Cambridge, MA). Wild-type, p53$^{+/-}$, p53$^{-/-}$, and iNOS$^{-/-}$ animals were used in subsequent experiments. Bleomycin (Bristol-Myers Squibb) was resuspended in 0.9% saline with or without antioxidants or benzyloxycarbonyl-Val-Ala-Asp fluoromethyl ketone (zVADfmk) and was administered via intratracheal instillation in a total volume that did not exceed 50 ml.

Isolation of Alveolar Macrophages. C57BL/6 mice were anesthetized with 60 mg/kg sodium phenobarbitol, and were exsanguinated by severing the dorsal artery. The lungs were removed and lavaged five times with 1.0 ml aliquots of PBS. Cells were recovered by centrifugation (1500 rpm for 5 min). Recovered cells (0.5×10^6 per mouse) were >95% macrophages and >99% viable as determined by trypan blue exclusion. Macrophages were cultured in MEM medium with 10% fetal bovine serum (GIBCO BRL).

DNA Fragmentation Analysis. Apoptosis was measured by propidium iodide (PI) staining for determination of the percentage of cells with subdiploid DNA content as described previously (18). Cells were harvested by centrifugation and incubated at 4°C for 24 h in PBS containing 50 μg/ml PI and 0.1% Triton X-100, and PI fluorescence was measured by FACS® (FACScan™; Becton Dickinson). Alternatively, oligonucleosomal DNA fragmentation ("DNA ladders") was detected by agarose gel electrophoresis. Cells were lysed in a buffer containing 0.5% Triton X-100, 20 mM EDTA, and 50 mM Tris (pH 8.0), and DNA fragments were harvested by centrifugation for 15 min at 12,000 *g* (19). The DNA in the supernatants was precipitated by addition of 2 vol isopropanol and NaCl (to 0.5 M final concentration) for 24 h at −20°C after addition of 2 vol isopropanol and NaCl (to 0.5 M final concentration). After centrifugation at 12,000 *g* for 10 min, precipitates were harvested, dried, and incubated for 1 h in TE buffer (10mM Tris [pH 8.0] and 1 mM EDTA] containing 0.2 mg/ml proteinase K and 1 mg/ml RNase A. The DNA fragments were resolved by electrophoresis for 1 h at 70 V on 1.5% agarose gels preimpregnated with ethidium bromide, and were detected by UV transillumination and photographed.

DNA Nick End Labeling of Tissue Sections. Lung sections were fixed by inflation with buffered 10% formalin solution and embedded in paraffin. Thin (4 μm) sections were prepared, and DNA fragmentation was analyzed by TdT-uridine nick end labeling (TUNEL [20]) using a commercial kit (Promega). Tissue sections were deparaffinized in xylene, rehydrated in alcohol, and transferred to PBS. Tissues were then fixed in 4% paraformaldehyde at room temperature for 5 min. Tissues were incubated with 20 μg/ml proteinase K for 10 min at room temperature. After two 5-min washes with PBS, tissues were preincubated with TdT buffer for 10 min at room temperature. TdT and buffer were then added to the tissue sections, and the slides were incubated in a humid atmosphere at 37°C for 1 h. EDTA (10 mM in water) was added to the tissues for 5 min to stop the reaction. The slides were washed three times (5 min each) with PBS, and in some experiments they were stained with 10 μg/ml PI for 10 min before they were washed again three times (5 min each) with PBS. Cover slips were mounted using Prolong (Molecular Probes). The slides were analyzed using an Olympus Inverted System Microscope IX70, and photographs were taken with a Nikon 35-mm camera.

Immunocytochemistry and Confocal Microscopy. Isolated alveolar macrophages were washed with PBS, fixed with 4% paraformaldehyde for 20 min at 4°C, and washed twice in PBS. Macrophages were mounted by cytospin, permeabilized with 0.2% Triton X-100 for 5 min at 4°C, and washed with PBS. Cells were blocked in a buffer containing 10% goat serum and 5% normal horse serum in PBS, incubated overnight at 4°C with a polyclonal sheep anti–mouse p53 antibody (pan-p53; Boehringer), diluted 1:80 in blocking buffer. Cells were washed once with PBS containing 0.01% Brij and twice with PBS (5 min each) before incubation with fluorescein-conjugated rabbit anti–sheep polyclonal secondary antibody (Cappel) diluted 1:200 in blocking buffer. Samples were analyzed using a Zeiss confocal laser scanning microscope (upright version) equipped with an argon and HeNe laser. Signals were collected by photomultipliers with a 590-nm (PI) long pass

[1]*Abbreviations used in this paper:* iNOS, inducible nitric oxide synthase; LSC, laser scanning cytometer; NAC, *N*-acetylcysteine; PI, propidium iodide; SNAP, *s*-nitrosoaminopereillamine; TUNEL, TdT-uridine nick end labeling.

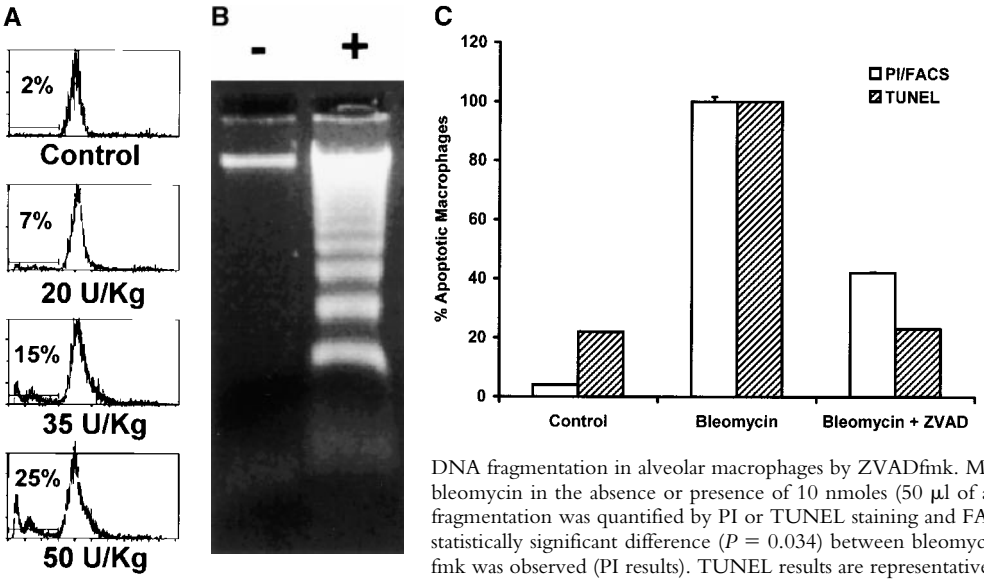

Figure 1. Bleomycin induces apoptosis of alveolar macrophages in vivo. (A) Cells were exposed to the indicated doses of bleomycin for 5 h in vivo, and DNA fragmentation was measured by PI staining and FACS® analysis as outlined in Materials and Methods. Results shown are of one experiment typical of three. (B) Bleomycin stimulates oligonucleosomal DNA fragmentation. Animals were treated for 5 h in vivo with vehicle or 50 U/kg bleomycin, and DNA fragmentation was analyzed by agarose gel electrophoresis. Results are representative of five experiments. (C) Inhibition of DNA fragmentation in alveolar macrophages by ZVADfmk. Macrophages were treated with 50 U/Kg bleomycin in the absence or presence of 10 nmoles (50 μl of a 200-μm stock) zVADfmk, and DNA fragmentation was quantified by PI or TUNEL staining and FACS® analysis (mean ± SEM, $n = 4$). A statistically significant difference ($P = 0.034$) between bleomycin alone versus bleomycin plus zVADfmk was observed (PI results). TUNEL results are representative of two experiments.

filter and a 520–560-nm (FITC) band pass filter, respectively. Digitized images were transmitted to a Macintosh-based image analysis system through a GPIB interface using BDS-LSM software (Biological Detection Systems). Composite images were assembled using Adobe Photoshop (Adobe Systems, Inc.).

Immunohistochemical Analyses. Formalin-fixed, paraffin-embedded sections (4 μm) were deparaffinized in xylene, rehydrated in alcohol, and transferred to PBS. Antigen retrieval was performed with target retrieval solution (Dako). Sections were washed three times with PBS (5 min each) and incubated for 20 min at room temperature with protein blocking solution containing 5% normal horse serum and 1% normal goat serum. The blocking solution was removed and the sections were incubated for 24 h at 4°C with a 1:400 dilution of rabbit polyclonal anti–mouse iNOS antibody (Transduction Laboratories) or a rabbit antipan cytokeratin antibody (Dako). Tissue sections were washed once with PBS containing 0.01% Brij and twice with PBS (5 min each). Sections were then incubated with protein blocking solution (above) for 10 min at room temperature. The blocking solution was removed, and the sections were incubated with a 1:400 dilution of FITC-conjugated goat anti–rabbit secondary antibody (Cappel) for 1 h at room temperature. Sections were washed once with PBS containing 0.01% Brij and twice with PBS (5 min each). Cell nuclei were stained with 10 mg/ml PI for 10 min and washed three times with PBS (5 min each). Cover slips were mounted using Prolong (Molecular Probes). Immunofluorescence microscopy was performed using a 40× objective (ZeissPlan-Neofluar) on an epifluorescence microscope equipped with narrow bandpass excitation filters mounted in a filter wheel (Ludl Electronic Products) to individually select for green and red fluorescence. Images were captured using a chilled CCD camera (Hamamatsu) on a PC computer. Images were further processed using Adobe Photoshop software (Adobe Systems).

Laser Scanning Cytometer Analysis. The laser scanning cytometer (LSC; CompuCyte Corporation) is an instrument designed to enable fluorescence-based quantitative measurements on tissue

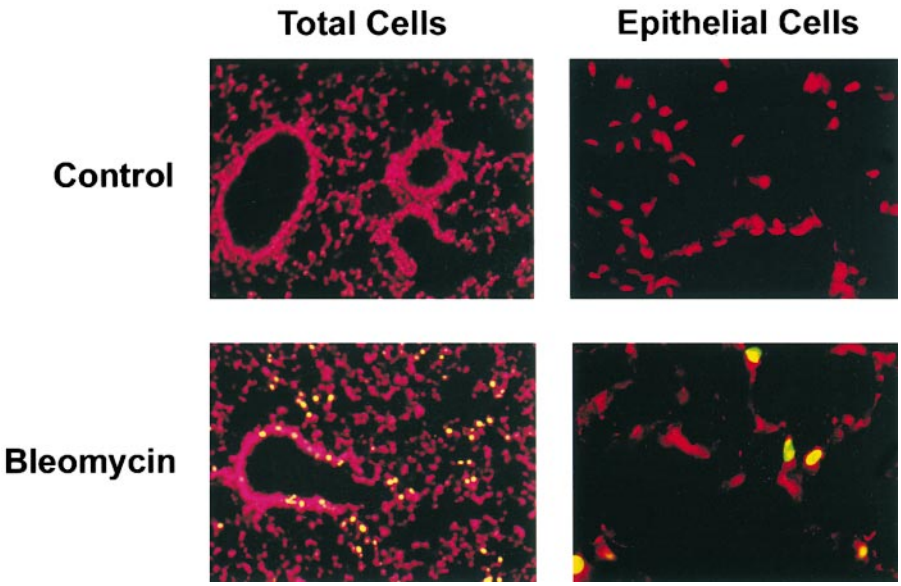

Figure 2. TUNEL analysis of lung tissues 5 h after instillation of 50 U/Kg bleomycin. Cells were counterstained with PI (total cells) or an antibody to cytokeratin (epithelial cells). TUNEL-positive cells appear green and yellow. Top panels, vehicle controls; bottom panels, bleomycin-treated lungs. Original magnification: ×20.

sections or other cellular preparations at the single cell level. The instrument consists of a base unit containing an Olympus BX50 fluorescent microscope and an optics/electronics unit coupled to argon and HeNe laser support elements and a computer. We used the instrument to determine the total number of TUNEL-positive, iNOS-positive, or cytokeratin-positive cells in whole lung sections. Cell nuclei in lung sections were first contoured by PI staining (red), and cells positive for iNOS or TUNEL were subsequently analyzed for emitted green fluorescence. The number of positive cells and the relative levels of green fluorescence within each cellular contour were automatically processed by CompuCyte software to generate a list of properties for that cell. Results are expressed as total number of cells expressing iNOS, cytokeratin, or TUNEL per mouse lung section and the mean level of iNOS expression per cell.

Statistical Analysis. All statistical analyses were performed with SPSS software. Values are presented as mean ± SEM. Experiments with statistical treatment included an independent sample *t* test. Differences between values were considered significant for $P < 0.05$.

Results

Bleomycin Induces Caspase-dependent DNA Fragmentation in the Lung. Previous work has shown that bleomycin can induce direct (double-strand) DNA scission (21). Because in situ measurements of apoptosis typically rely on the detection of DNA strand breaks, we first analyzed the nature of bleomycin-induced DNA fragmentation in alveolar macrophages. Animals were dosed with various concentrations of bleomycin via intratracheal instillation, and apoptosis was measured by PI or TUNEL staining and FACS® analysis. Bleomycin-induced DNA fragmentation was dose dependent (Fig. 1 A) and involved production of typical oligonucleosome-length DNA fragments, visualized by agarose gel electrophoresis (Fig. 1 B). Importantly, DNA fragmentation was significantly blocked by the pancaspase inhibitor, zVADfmk, whether measured by PI or TUNEL staining and FACS® analysis (Fig. 1 C). These data demonstrate that bleomycin-induced DNA fragmentation is secondary to apoptosis and is not due to a direct action of the drug on DNA.

Parallel TUNEL analysis of apoptosis in situ revealed diffuse staining throughout the lung parenchyma (Fig. 2). Immunofluorescence two-color analysis of cell death in bronchiolar and alveolar epithelial cells by cytokeratin plus TUNEL staining confirmed that bleomycin stimulated extensive apoptosis in these cells (Fig. 2). Together, these data suggest that bleomycin stimulates apoptosis in multiple cell types within the lung.

Bleomycin-induced p53 Activation Is Dependent on Reactive Oxygen Species in the Lung. Apoptosis induced by bleomycin and other DNA damaging agents occurs via a p53-dependent pathway in many model systems (6). Activation of p53 involves translocation of the protein from the cytoplasm to the nucleus (22). We therefore measured this phenomenon as a surrogate for p53 activation in alveolar macrophages exposed to bleomycin in vivo or in vitro. In our experiments, p53 was visualized with a fluorescein-conjugated secondary antibody, and nuclei were detected by staining with PI. In vehicle-treated cells, p53 was uniformly restricted to the cytosol, as demonstrated by non-overlapping green and red fluorescence (Fig. 3 A). After exposure to bleomycin in vivo, p53 rapidly translocated to the nucleus, detected by the appearance of overlapping green and red fluorescence (yellow) in the cells (Fig. 3 A). Interestingly, exposure of isolated alveolar macrophages to bleomycin in vitro had no effect on the subcellular localization of p53, which remained entirely cytosolic (Fig. 3 B). These results strongly suggest that p53 is activated by bleomycin in alveolar macrophages exposed to the drug in vivo, but not in vitro.

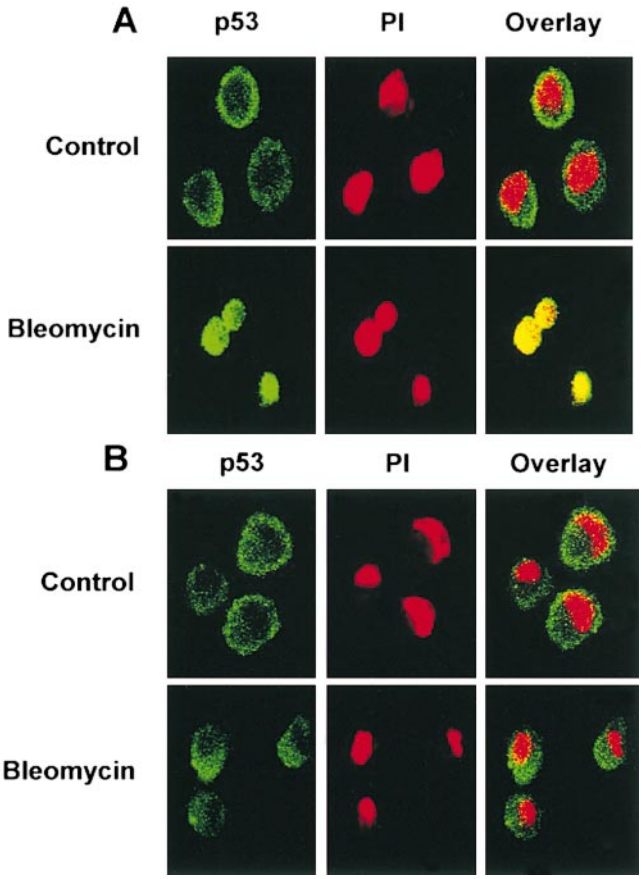

Figure 3. Confocal laser scanning microscopy analysis of p53 localization after bleomycin exposure. (A) Effects of in vivo exposure. Animals were treated for 5 h with 50 U/kg bleomycin, and subcellular p53 localization was determined in isolated alveolar macrophages by immunofluorescence as described in Materials and Methods. p53 was detected with FITC (green fluorescence); nuclei were visualized by staining for DNA with PI (red fluorescence). Note that bleomycin exposure caused relocalization of p53 from the cytosol to the nucleus (bottom panels), whereas p53 remained confined to the cytosol in vehicle-treated controls. (B) Effects of in vitro exposure. Macrophages were isolated by lavage and treated with 1.6 U/ml bleomcyin or vehicle (control) for up to 5 h. Cells were then stained with anti-p53 (green fluorescence) and PI (red fluorescence). Note that p53 is confined to the cytoplasm in both the control and bleomycin-treated cells. Images are representative of a field captured by microscopy, and results are representative of three experiments. Original magnification: ×63.

The p53 localization results indicated that factor(s) present within the lung microenvironment play a critical role in promoting bleomycin-induced p53 activation. Oxygen radicals and oxidative stress are known to exert strong effects on both lung physiology and p53 function. To address the involvement of reactive oxygen species in p53 activation, we exposed mice to bleomycin in the absence or presence of the thiol antioxidant, *N*-acetylcysteine (NAC) in vivo, isolated the macrophages by lavage, and monitored p53 localization by immunofluorescence confocal microscopy. NAC (200 nmoles) completely suppressed bleomycin-induced translocation of p53 to the nucleus (Fig. 4 A; compare middle and right panels). Furthermore, NAC enhanced bleomycin-induced DNA fragmentation threefold in alveolar macrophages, as measured by PI staining and FACS® analysis (Fig. 4 B). Other antioxidants (α-tocopherol, ascorbate) also potentiated apoptosis (data not shown).

We next attempted to reconstitute nuclear translocation by exposing alveolar macrophages to various oxidants in vitro. Incubation with the NO donor, *s*-nitrosoaminopereillamine (SNAP [10 mM]), had no effect on nuclear p53 localization on its own (Fig. 5). However, incubation with SNAP plus bleomycin (1.6 U/ml) led to strong nuclear translocation of p53 (Fig. 5). Together, these data strongly suggest that reactive oxygen species, and in particular NO, are required for bleomycin-induced p53 activation in lung cells.

Increased Bleomycin-induced Apoptosis in p53$^{-/-}$ Animals. Gene-deficient (p53$^{-/-}$) mice have been used in previous studies to establish an unambiguous cause–effect relationship between p53 expression and apoptosis (23, 24). Therefore, we measured bleomycin-induced apoptosis in alveolar macrophages from wild-type or p53$^{-/-}$ mice to directly determine p53's involvement in the response. No differences in the kinetics or magnitude of apoptosis were observed in the cells incubated with bleomycin in vitro (Fig. 6 A). Strikingly, however, intratracheal instillation of bleomycin led to significantly enhanced (twofold higher; $P < 0.05$) levels of apoptosis in p53$^{-/-}$ macrophages compared with wild-type controls (Fig. 6 B). In addition, analysis of DNA fragmentation in whole lung tissue by TUNEL confirmed that more apoptotic cells were present in the lungs of the p53-deficient animals (Fig. 6 C). To quantify the levels of DNA fragmentation observed, we employed LSC. The LSC is an instrument in which tissue sections that are mounted on a solid surface (i.e., a glass microscope slide) are interrogated by a 5-μm diameter argon laser that repeatedly scans along a line as the surface is moved past it on a computer-controlled motorized stage. TUNEL and/or immunostained cell preparations are then contoured by light scatter or counterstain-

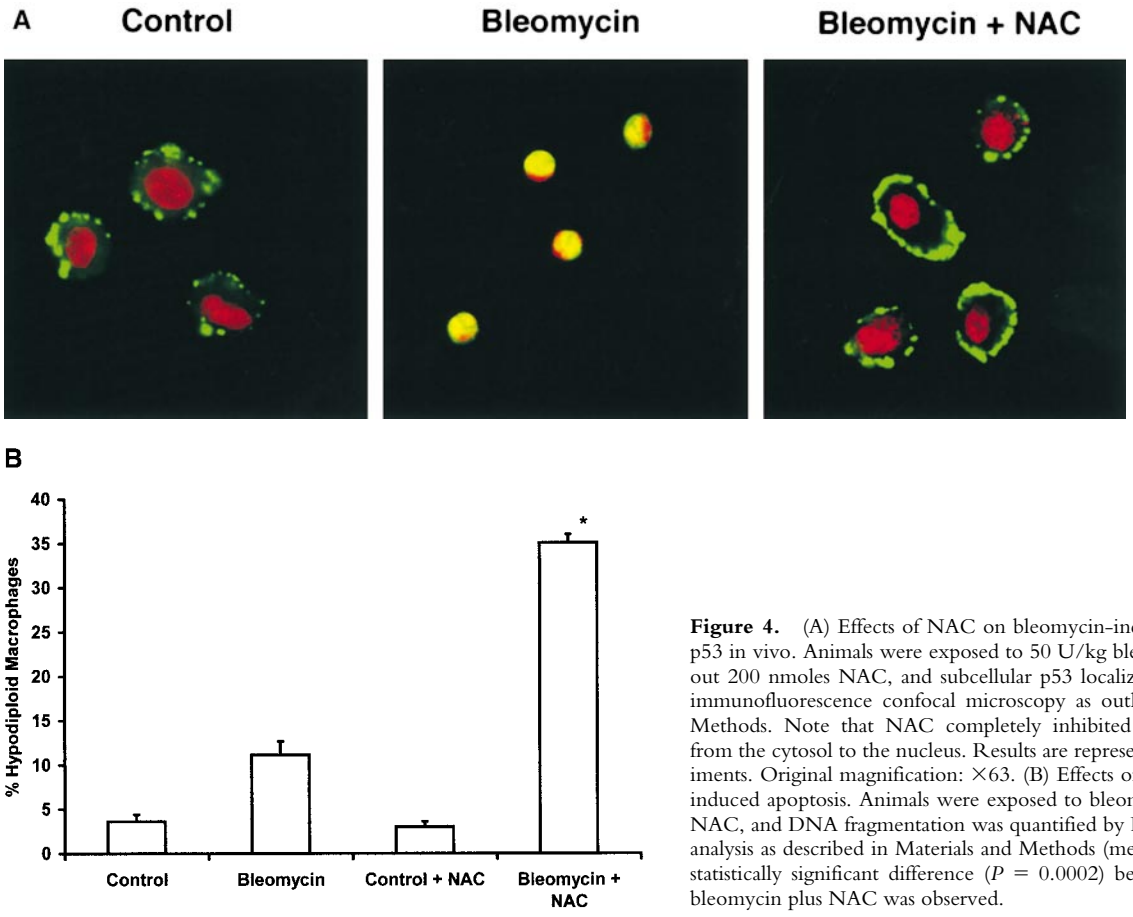

Figure 4. (A) Effects of NAC on bleomycin-induced relocalization of p53 in vivo. Animals were exposed to 50 U/kg bleomycin with or without 200 nmoles NAC, and subcellular p53 localization was analyzed by immunofluorescence confocal microscopy as outlined in Materials and Methods. Note that NAC completely inhibited relocalization of p53 from the cytosol to the nucleus. Results are representative of three experiments. Original magnification: ×63. (B) Effects of NAC on bleomycin-induced apoptosis. Animals were exposed to bleomycin with or without NAC, and DNA fragmentation was quantified by PI staining and FACS® analysis as described in Materials and Methods (mean ± SEM, $n = 3$). A statistically significant difference ($P = 0.0002$) between bleomycin and bleomycin plus NAC was observed.

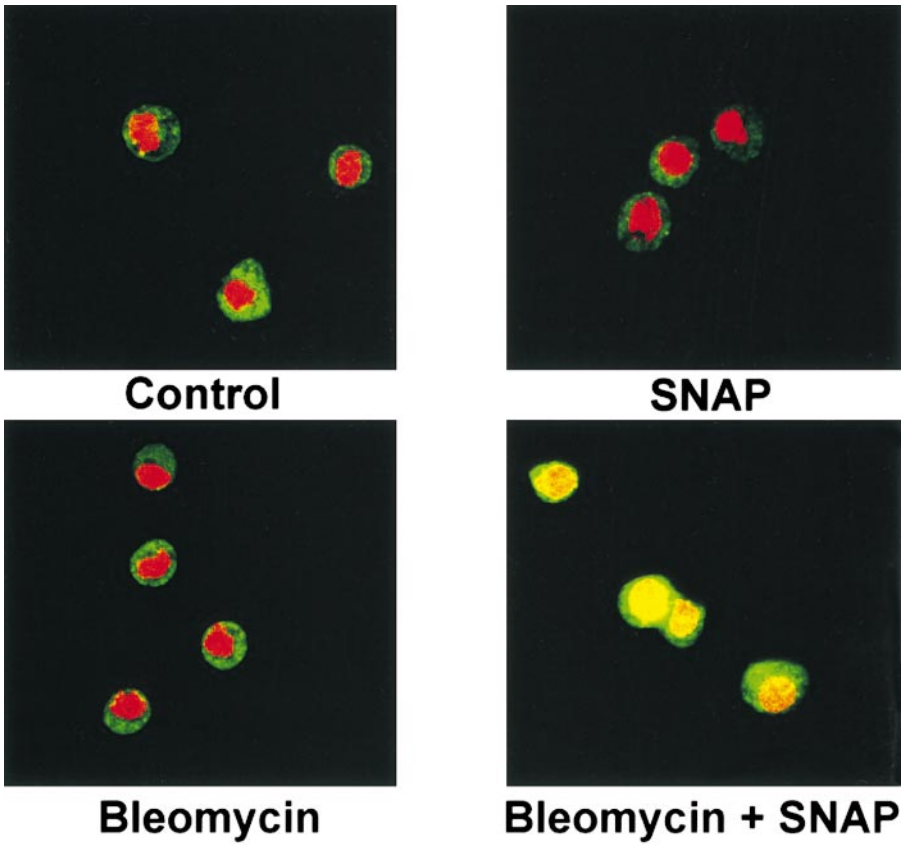

Figure 5. An NO donor promotes bleomycin-induced p53 activation in vitro. Alveolar macrophages were isolated from wild-type mice by lavage. Cells were treated with vehicle (control), SNAP (10 mM), bleomycin (1.6 U/ml), or bleomycin plus SNAP, and p53 localization was analyzed at 5 min as described in Materials and Methods. Note that bleomycin plus SNAP induced relocalization of p53 from the cytoplasm to the nucleus, whereas bleomycin or SNAP did not.

ing with a specific fluorescent dye, and fluorescence emissions within the contours are automatically processed by the software to generate a list of properties for the cells within that tissue. Thus, the LSC can be used very much like FACS® to obtain two- and three-color fluorescence intensity information from a heterogeneous tissue specimen. LSC-guided contour analysis demonstrated homogeneous distribution of apoptotic cells throughout all lobes of the lung (Fig. 6 D), and direct quantification of TUNEL-positive cells in whole lung sections confirmed that rates of apoptosis were about twofold higher in the $p53^{-/-}$ lungs compared with controls (Fig. 6 E). Furthermore, analysis of epithelial cell apoptosis suggested that levels of cell death were also elevated in this subpopulation in the $p53^{-/-}$ mice (Fig. 6 F). Levels of bleomycin-induced apoptosis were indistinguishable in wild-type and $p53^{+/-}$ cells (data not shown), indicating that a gene dosage effect is not involved.

p53 Activation Is Dependent on iNOS. Our preliminary results (Fig. 5) and published reports in the literature (9, 25, 26) suggested that NO can promote p53 activation. We therefore analyzed bleomycin-induced nuclear p53 localization in alveolar macrophages from wild-type and $iNOS^{-/-}$ mice. Intratracheal bleomycin instillation led to strong p53 activation in wild-type cells, but this effect was completely absent in cells from the NOS-$2^{-/-}$ animals (Fig. 7 A). Furthermore, DNA fragmentation was considerably elevated in the NOS-$2^{-/-}$ lungs as determined by TUNEL staining (Fig. 7 B). LSC contour mapping confirmed diffuse apoptosis throughout the lung (Fig. 7 C), and LSC-mediated quantification of cell death confirmed that the levels of TUNEL-positive cells were about twofold higher in the NOS-$2^{-/-}$ lungs compared with controls (Fig. 7 D). In subsequent experiments, we analyzed the effects of bleomycin on iNOS expression in wild-type mice. Bleomycin induced an increase in iNOS-positive cells within 5 h (Fig. 8 A), and LSC analysis revealed an approximately twofold increase in the number of positive cells (Fig. 8 B). However, analysis of fluorescence intensity demonstrated that the level of iNOS expression was similar in untreated and bleomycin-treated cells (Fig. 8 C).

Our overall hypothesis is that impaired clearance of apoptotic debris serves as a trigger for inflammation in the early stages of lung injury. This hypothesis predicts that levels of inflammation would be substantially higher in the $iNOS^{-/-}$ and $p53^{-/-}$ mice compared with wild-type controls because of increased cell death. Consistent with this idea, chronic exposure to bleomycin led to marked increases in inflammatory infiltrate and disruption of alveolar architecture in the $iNOS^{-/-}$ and $p53^{-/-}$ mice compared with wild-type littermates (Fig. 9). Increased inflammation was obvious by 7 d after exposure and persisted up to 14 d, at which point the $iNOS^{-/-}$ and $p53^{-/-}$ mice died with high frequency (Fig. 9, and data not shown). These data strongly support roles for iNOS and p53 in suppressing inflammation in this model system.

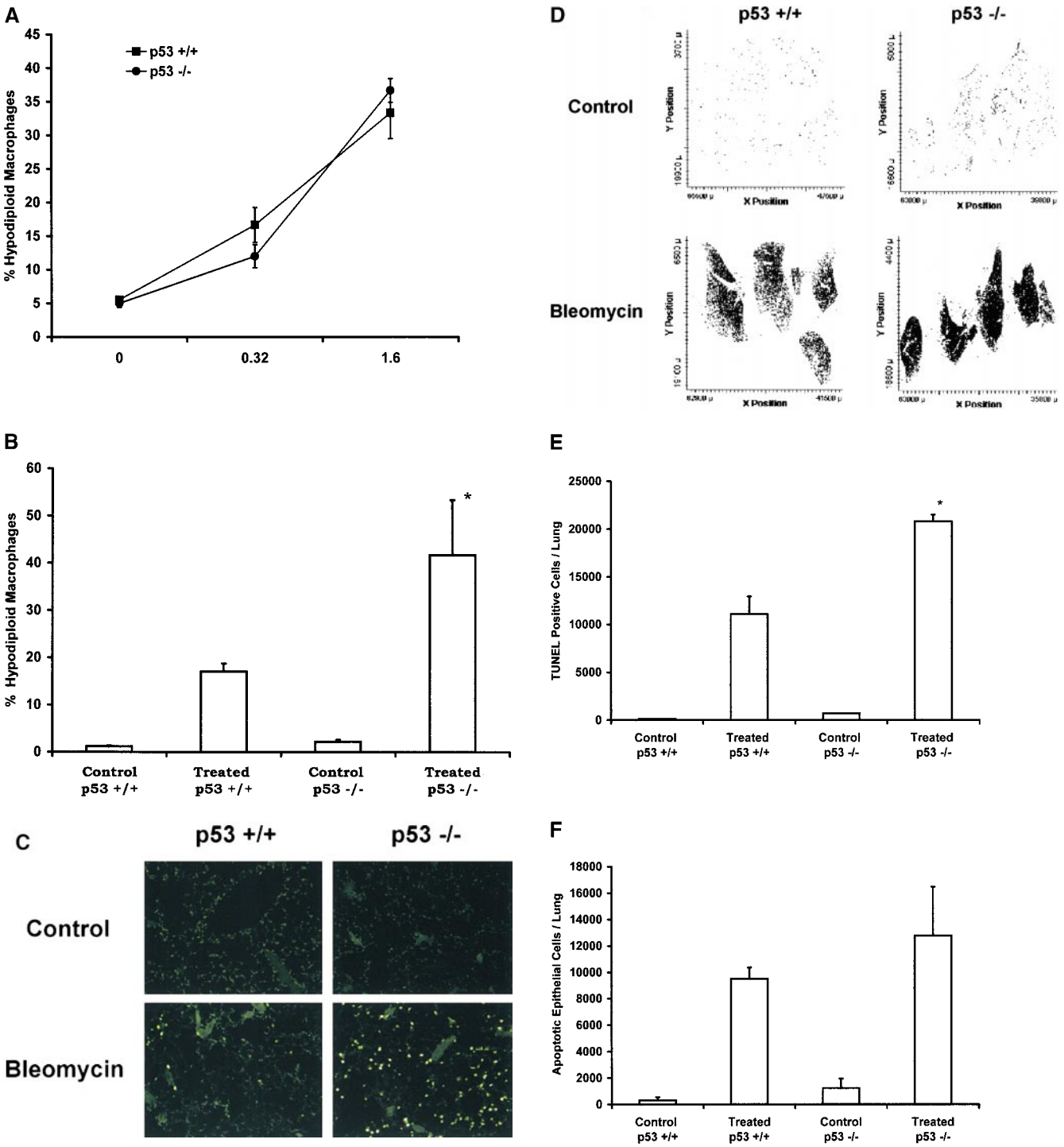

Figure 6. Comparison of bleomycin-induced apoptosis in wild-type and $p53^{-/-}$ cells. (A) Effects of bleomycin on alveolar macrophages in vitro. Cells isolated from wild-type or p53-deficient C57BL/6 littermates were treated with 0.32 U/ml or 1.6 U/ml bleomycin for 5 h, and DNA fragmentation was measured by PI staining and FACS® analysis (mean ± SEM, $n = 3$). (B) Effects of bleomycin on alveolar macrophages in vivo. Wild-type and $p53^{-/-}$ mice were exposed to 50 U/kg bleomycin for 5 h in vivo, and DNA fragmentation in isolated alveolar macrophages was measured by PI staining and FACS® analysis (mean ± SEM, $n = 3$). A statistically significant difference ($P < 0.05$) between the responses measured in cells from $p53^{+/+}$ and $p53^{-/-}$ mice was observed. (C) TUNEL analysis of bleomycin-induced apoptosis in situ. Animals were exposed to vehicle or 50 U/kg bleomycin for 5 h, and apoptosis was analyzed by TUNEL staining as described in Materials and Methods. Original magnification: ×20. (D) Localization of apoptotic cells in situ. TUNEL-stained slides from untreated or bleomycin-treated lungs were analyzed for distribution of apoptotic cells by LSC. Results are representative of three independent experiments. (E) Quantification of apoptosis in situ. Apoptotic cells were counted in whole lung sections by LSC. Results are expressed as mean values ± SEM from sections obtained from three independent animals. A statistically significant difference ($P < 0.05$) between $p53^{+/+}$ and $p53^{-/-}$ lungs was observed. (F) Quantification of epithelial cell apoptosis in situ. Epithelial cell apoptosis was measured by two-color TUNEL plus cytokeratin staining as outlined in Materials and Methods. Results are from two separate experiments.

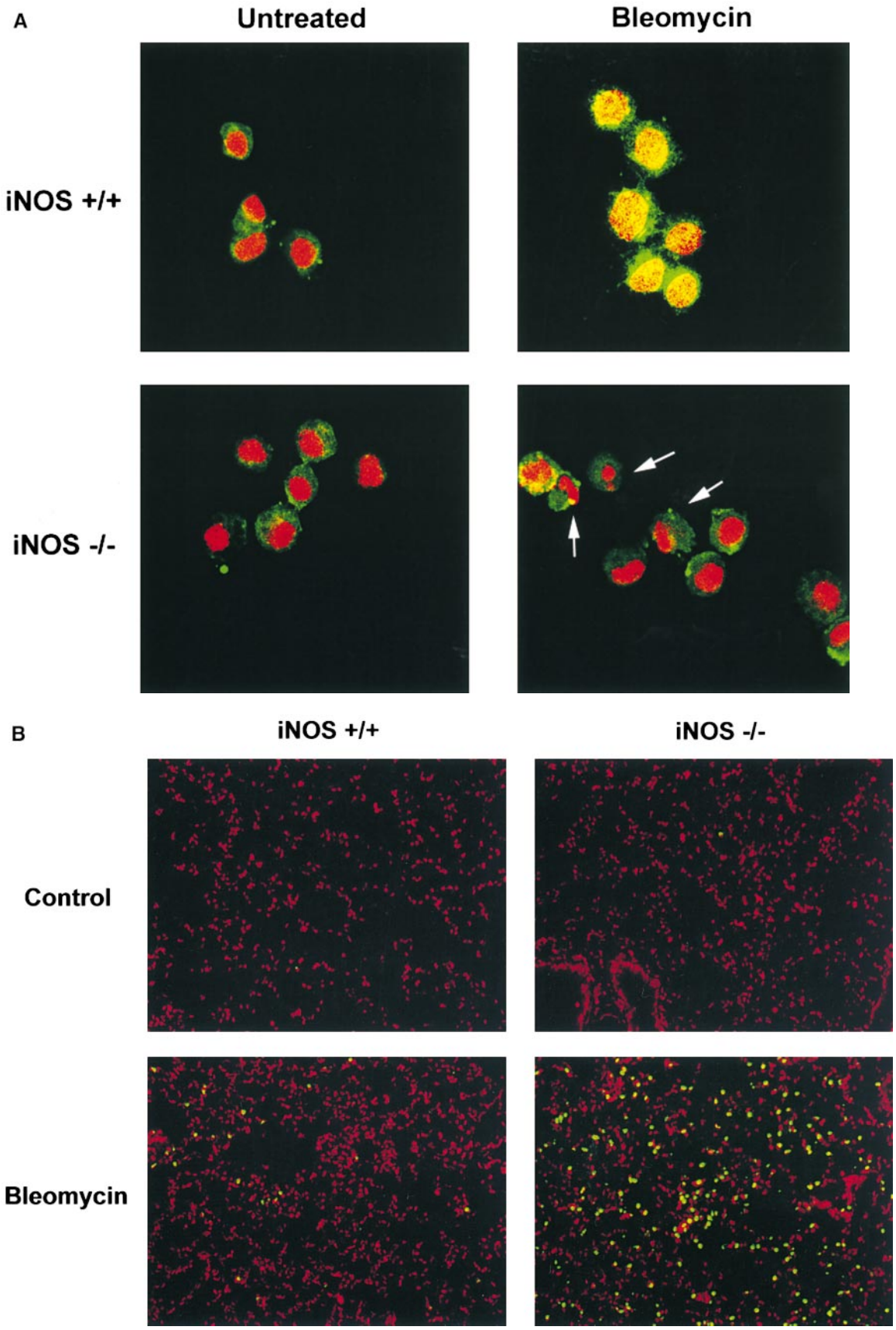

Figure 7. *(continues on facing page).*

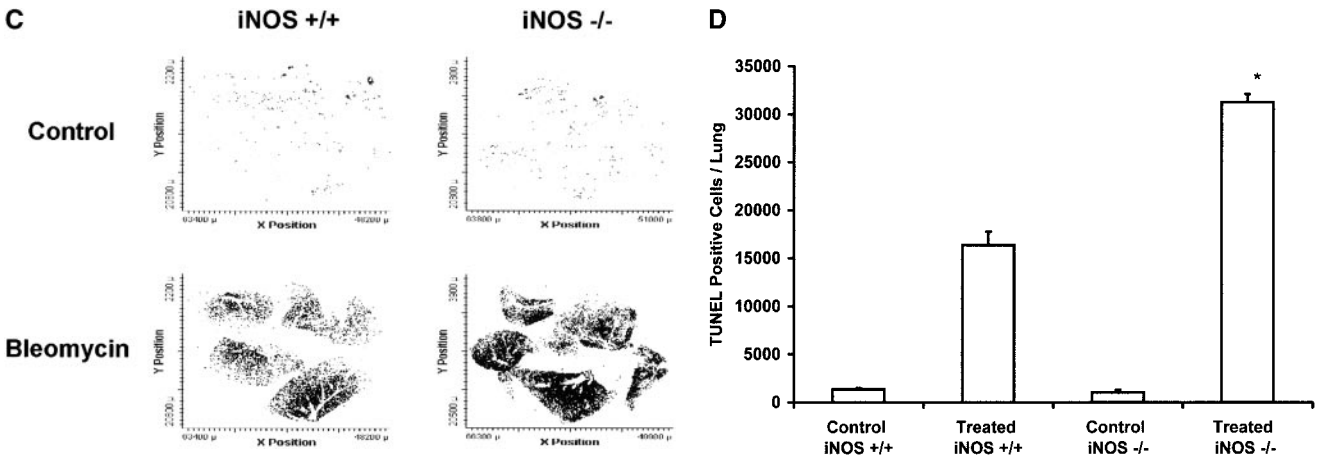

Figure 7. (A) iNOS is required for bleomycin-induced p53 activation in vivo. Wild-type and NOS-2$^{-/-}$ mice were exposed to bleomycin via intratracheal instillation. After 2 h, alveolar macrophages were isolated by lavage, and nuclear p53 localization was analyzed by confocal microscopy. Note strong nuclear p53 localization in cells from the iNOS$^{+/+}$ animals that is absent from the iNOS$^{-/-}$ cells. Arrows indicate treated iNOS$^{-/-}$ macrophages exhibiting apoptotic morphological changes. (B) TUNEL staining for apoptosis in situ. Animals were exposed to vehicle or 50 U/kg bleomycin for 5 h, and apoptosis was analyzed by TUNEL staining. Original magnification: ×20. (C) Localization of apoptotic cells in situ. TUNEL-stained slides from untreated or bleomycin-treated lungs were analyzed for distribution of apoptotic cells by LSC. Results are representative of three independent experiments. (D) Quantification of apoptosis in situ. Apoptotic cells were counted in whole lung sections by LSC. Results are expressed as mean values ± SEM from sections obtained from three independent animals. A statistically significant difference ($P = 0.005$) between wild-type and iNOS$^{-/-}$ lungs was observed.

Discussion

The p53 tumor suppressor protein plays a central role in the cellular response to DNA damage, mediating a cell cycle checkpoint that leads to growth arrest or apoptosis. Recent work has demonstrated that apoptosis is one of the earliest pulmonary alterations detected in mice exposed to fibrogenic stimuli (27), and it has been suggested that cell death can directly contribute to inflammation in other tissue model systems (i.e., the kidney; reference 14). Given that most (if not all) of the known stimuli for pulmonary fibrosis induce DNA damage, we speculated that p53 would participate in the effects of bleomycin. To begin to address this possibility, we analyzed the effects of bleomycin on p53 activation and apoptosis in alveolar macrophages and other lung cell types in wild-type and p53$^{-/-}$ C57BL/6 mice. As expected, exposure of macrophages to bleomycin in vivo led to rapid translocation of p53 from the cytoplasm to the nucleus, consistent with p53 activation. Interestingly, parallel immunoblotting experiments demonstrated that p53 levels did not rise substantially (data not shown), suggesting that posttranslational mechanisms (i.e., phosphorylation; reference 28) are probably involved.

Almost all published reports on the involvement of p53 in apoptosis have focused on its ability to promote cell death in response to DNA damage (23, 24, 29, 30). For this reason, we expected that bleomycin-induced apoptosis would be attenuated or absent in cells derived from p53$^{-/-}$ mice. Unexpectedly, however, levels of apoptosis were significantly elevated in the p53$^{-/-}$ mice compared with wild-type controls. To our knowledge, ours is the first description of a p53-dependent survival pathway in the lung. Although unanticipated, previous work has shown that the role of p53 in DNA damage–induced apoptosis is tissue and cell type dependent (31), and p53-dependent inhibition of apoptosis has even been documented previously in another model system (32). Our explanation for this apparent paradox is that in our system, activation of p53 results in transactivation of prosurvival genes, whereas in thymocytes and certain other tissues, p53 induces the expression of proapoptotic genes (Bax, Fas). More specifically, it is possible that the p53 target, p21/WAF1, plays an important role in promoting cell survival in response to exposure to DNA damaging agents in the lung. Recent studies have shown that p21 inhibits apoptosis in monocytes and other cell types by a mechanism that may involve inhibition of stress-activated protein kinase(s) (33, 34). Levels of p53 and p21 are increased in lung tissue from patients with idiopathic pulmonary fibrosis (35), suggesting that the stress response pathway is activated in the disease. Accumulation of apoptotic debris in the p53$^{-/-}$ mice may also be linked to reduced expression of thrombospondin, a p53-regulated gene (36) that is required for some pathways of apoptotic cell clearance by phagocytic cells (37). Interestingly, thrombospondin-1$^{-/-}$ mice exhibit pathological changes within the lung consistent with inflammation (38), suggesting that impaired clearance may exacerbate inflammation. We speculate that p21, thrombospondin, and possibly other targets of p53 play important roles in protecting the lung from inflammation. Importantly, the C57BL/6 mouse strain used in our study is considered fibrosis prone, whereas other strains (i.e., Balb/c) are resistant. Once other strains of p53-deficient mice are available, it will be important to determine whether or not p53's ability to inhibit apoptosis in the lung is mouse strain dependent.

An alternative interpretation of our results is that the TUNEL method detects DNA damage due to direct bleomycin-induced strand scission, and that the elevated

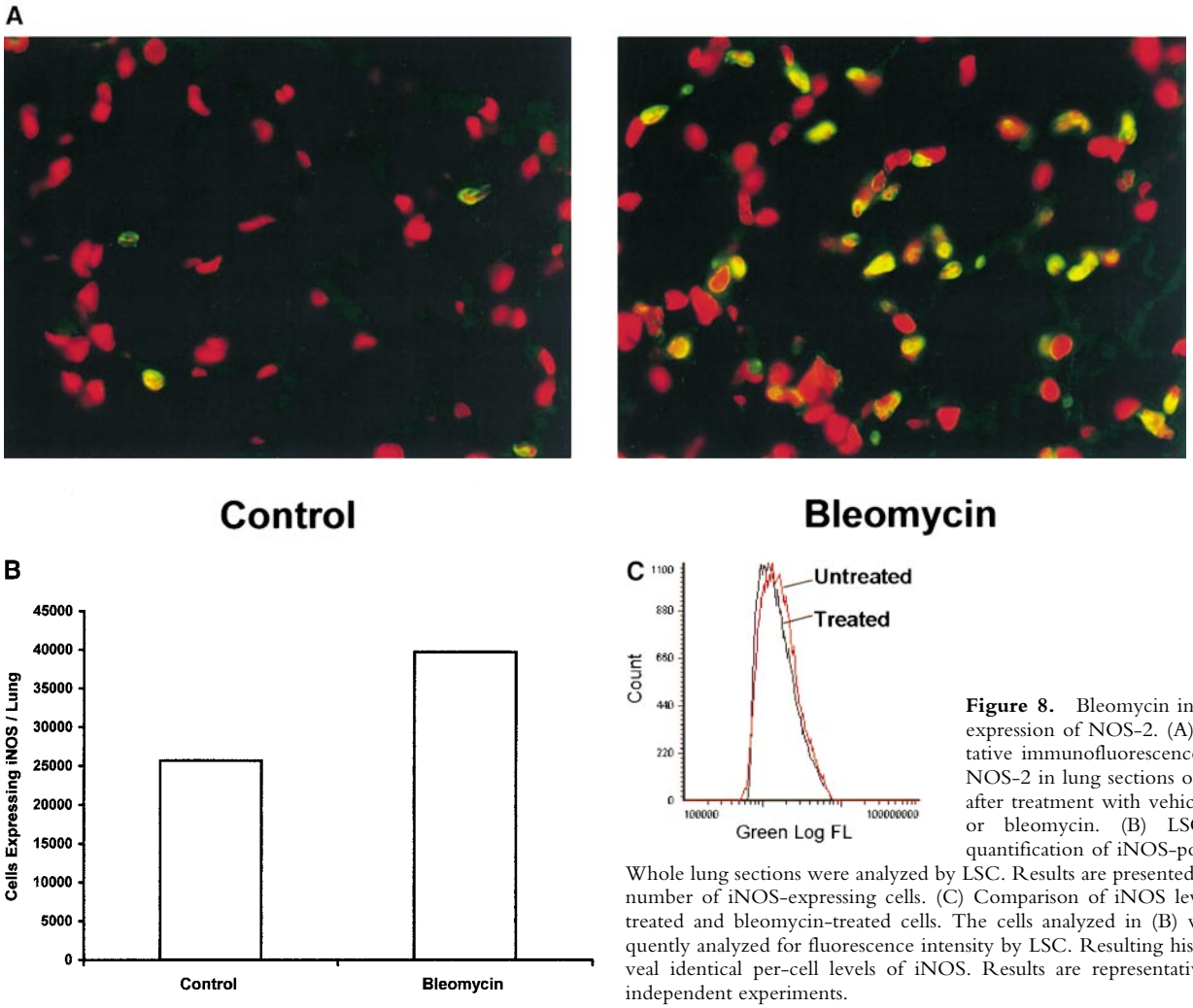

Figure 8. Bleomycin induces rapid expression of NOS-2. (A) Representative immunofluorescence images of NOS-2 in lung sections obtained 5 h after treatment with vehicle (control) or bleomycin. (B) LSC-mediated quantification of iNOS-positive cells. Whole lung sections were analyzed by LSC. Results are presented as the total number of iNOS-expressing cells. (C) Comparison of iNOS levels on untreated and bleomycin-treated cells. The cells analyzed in (B) were subsequently analyzed for fluorescence intensity by LSC. Resulting histograms reveal identical per-cell levels of iNOS. Results are representative of three independent experiments.

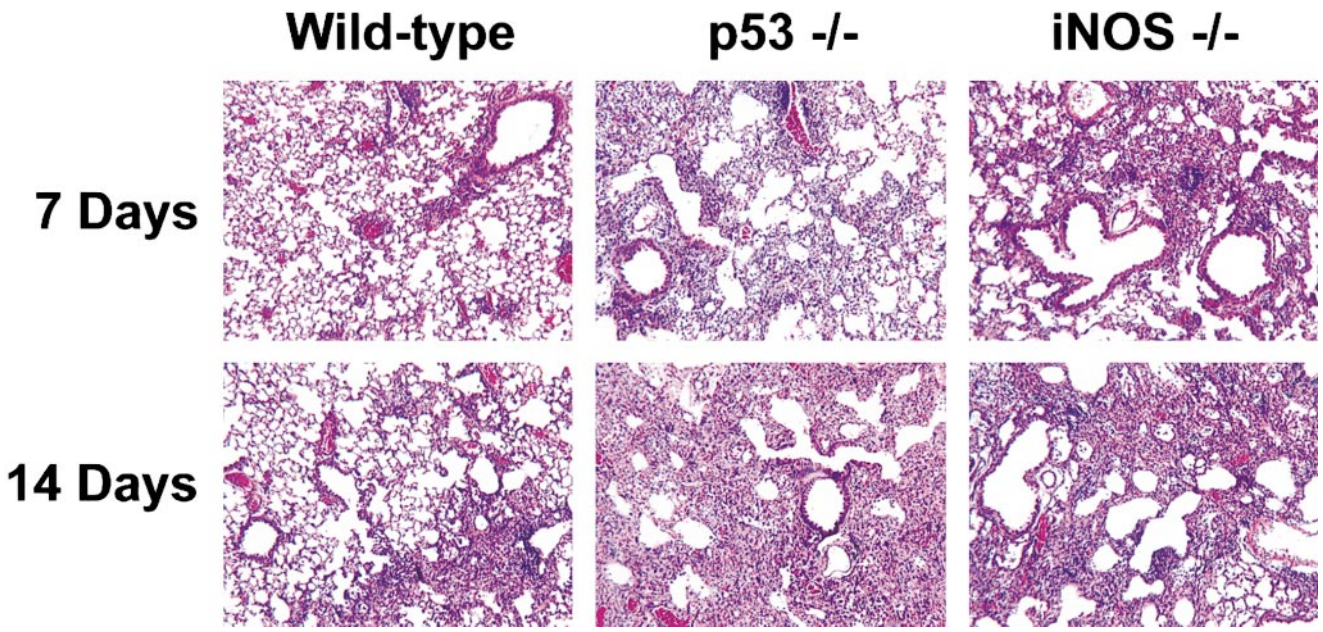

Figure 9. Increased bleomycin-induced inflammation in iNOS$^{-/-}$ and p53$^{-/-}$ mice. Animals were treated with 2.5 U/kg bleomycin via intratracheal administration. At the times indicated, animals were killed and inflammation was assessed by histological analysis after hematoxylin and eosin staining. Note profound inflammatory infiltrate by 7 d in the iNOS- and p53-deficient lungs. Indistinguishable results were observed in each of two animals at each time point.

TUNEL levels observed in the $p53^{-/-}$ animals are due to the absence of a p53-mediated mechanism that can repair this damage. This explanation was offered by another group who reported very similar increases in TUNEL-positive cells in $p53^{-/-}$ animals exposed to bleomycin in vivo (39). Although we considered this possibility very seriously, we have discounted it for several reasons. First, the pattern of DNA fragmentation induced by bleomycin was characteristic of apoptosis (Fig. 1 B) and not characteristic of the direct (random) effects of bleomycin on DNA (40, 41). This DNA fragmentation also took much longer to develop (between 1 and 2 h) than the kinetics of direct strand scission (essentially complete in minutes; reference 40). Second, the bleomycin-induced DNA fragmentation we measured in all of our assays was completely suppressed by zVADfmk (Fig. 1 C), indicating that it occurs via a caspase-dependent mechanism. Finally, recent work by Wyllie and colleagues (42–44) has shown that DNA damage induced by ionizing radiation is repaired equally well in $p53^{+/+}$ and $p53^{-/-}$ cells. The emergence of mutation-bearing cells in the $p53^{-/-}$ background is linked more closely to the inability of the cells to engage the apoptotic pathway than to defects in DNA repair, and apoptosis occurs well after all of the initial DNA damage has been repaired.

Comparison of p53 localization after exposure of alveolar macrophages to bleomycin in vitro and in vivo demonstrated that p53 activation was strictly dependent on factor(s) within the lung microenvironment. Our subsequent experiments established a central role for reactive oxygen species, and in particular NO, in this response. Initially, we found that the thiol antioxidant, NAC, blocked p53 activation, a result that is consistent with a role for reactive oxygen species in the response. A search for candidate mediator(s) demonstrated that NO donors can substitute for the lung microenvironment to promote p53 activation in vitro. Our studies with macrophages isolated from NOS-$2^{-/-}$ mice confirmed that iNOS is required for bleomycin-mediated p53 activation in vivo. A role for NO in p53 activation is well established (9), although the biochemical mechanism(s) involved remain unclear. One previous study presented evidence that NO promotes stabilization of p53 via inhibition of proteasome-mediated degradation of the protein (25), and another recent study suggests that NO can directly nitrosylate tyrosine residues in p53 (45). The data demonstrating bleomycin-induced nuclear p53 relocalization strongly suggest that protein stabilization alone does not explain the effects of NO on p53 function. Notably, proteasome inhibitors, which block p53 degradation in most cell types, do not promote p53 phosphorylation or nuclear relocalization by themselves (our unpublished observations).

One potential caveat of our experiments is that NOS-2 has been difficult to demonstrate in human macrophages (46). In this sense, the mouse alveolar macrophage may not serve as a perfect model for the corresponding human cells. However, it is possible that in response to lung injury, human alveolar macrophages (or some other resident cell type) generate NO via the action of a different NOS isozyme(s) (cNOS or eNOS). Alternatively, it is also conceivable that the lack of significant iNOS expression renders the human lung more fibrosis prone compared with the mouse lung.

The observation that bleomycin exposure leads to marked increases in inflammation in the $iNOS^{-/-}$ and $p53^{-/-}$ mice (Fig. 9) supports our hypothesis that p53 acts as a suppressor of inflammation in the lung through its ability to inhibit apoptosis. However, as noted above, the C57BL/6 mice are considered fibrosis prone, perhaps because they mount a strong Th1-type response (as opposed to a Th2 response) when challenged with proinflammatory stimuli or because their responses to DNA damage are unique. It will be of more interest to determine whether or not p53 protects the human lung from inflammatory injury. Patients with Li-Fraumeni syndrome possess germline defects in the p53 gene that lead to increased cancer susceptibility (47). To our knowledge, no study has investigated the possible relationship between expression of mutant p53 and propensity to develop pulmonary fibrosis, but our data would predict that these patients would exhibit increased susceptibility. In addition, it is possible that individual differences in T cell response patterns will play a significant role in disease susceptibility.

Although the effects of fibrogenic agents almost certainly involve reactive oxygen species, the effects of antioxidants on the development of pulmonary inflammation and fibrosis appear complex. Our data indicate that NO acts in a stress response pathway that counteracts bleomycin-induced cell death at the earliest stages of the response. However, abundant evidence is available indicating that chronic treatment with thiol antioxidants can partially inhibit bleomycin-induced lung injury (10, 48). It is clear that the tissue-damaging effects of neutrophils and basophils involve generation of superoxide and other reactive oxygen species. In addition, antioxidants can also inhibit the transcription factor, nuclear factor κB, which plays a central role in the inflammatory cytokine networks involving TNF-α and IL-1β (49). It should be noted that some studies have shown that NAC does not attenuate lung injury, and one report argued that the antioxidant exacerbated inflammation (50). Inhibition of apoptosis by oxidative stress has been linked to inhibition of caspase activation in other model systems (51), and our results suggest that oxidative stress is also involved in promoting p53's antiinflammatory effects in the lung. Direct analysis of particular redox-sensitive pathways will be required to determine the relative importance of each of these candidate mechanisms.

Our data support the emerging idea that early apoptosis contributes to inflammatory lung injury (27, 52–54), but precisely how it does so remains unclear. One attractive hypothesis is that the death of resident alveolar macrophages leads to loss of the balance between immunosuppressive and proinflammatory cell types within the lung. Although both resident and inflammatory macrophages can ingest apoptotic debris, the former never leave the tissue and are cleared by neighboring cells, whereas the latter migrate to draining lymph nodes (55), where they may promote antigen presentation and T cell activation. In fact, terminally differentiated macrophages can directly suppress

T cell activation (56) by competing with resident dendritic cells for engulfment of the apoptotic debris that serves as the source of antigens for presentation (15). Furthermore, resident tissue macrophages play a critical role in clearing neutrophils (57). Neurophils have an extremely short half-life, and recent work by Haslett and colleagues (58) has shown that levels of neutrophil influx correlate well with the extent of pulmonary fibrosis in several models of the disease (58). Additional effort is required to determine precisely how apoptotic cell clearance regulates tolerance to self-antigens within the lung.

The authors would like to thank Dr. Hiroki Kuniyasu (Department of Pathology, Hiroshima University School of Medicine, Hiroshima, Japan), and Dr. Corazon Bucana (Department of Cancer Biology, U.T. M.D. Anderson Cancer Center) for helping with lung histological analyses. The authors also thank Drs. David Menter (Department of Clinical Cancer Prevention, U.T. M.D. Anderson Cancer Center) and Michael Andreeff (Department of Molecular Hematology and Therapy, U.T. M.D. Anderson Cancer Center) for the use of their microscopes.

This work was supported by a grant from the National Heart, Lung, and Blood Institute (HL60537) and by the confocal microscopy and image analysis component of the cancer center support grant (CA16672). D. Davis was supported by a grant from the National Institute of Environmental Health and Safety (T32-ES07290).

Submitted: 22 February 2000
Revised: 24 May 2000
Accepted: 16 June 2000

References

1. Crystal, R.G., P.B. Bitterman, S.I. Rennard, A.J. Hance, and B.A. Keogh. 1984. Interstitial lung diseases of unknown cause. Disorders characterized by chronic inflammation of the lower respiratory tract. *N. Engl. J. Med.* 310:235–244.
2. V.T. DeVita, Jr., S. Hellman, and S.A. Rosenberg. 1993. Cancer: Principles & Practice of Oncology. 4th ed. J.B. Lippincott Company, Philadelphia. 2747 pp.
3. Jules-Elyse, K., and D.A. White. 1990. Bleomycin-induced pulmonary toxicity. *Clin. Chest Med.* 11:11–20.
4. Kastan, M.B., O. Onyekwere, D. Sidransky, B. Vogelstein, and R.W. Craig. 1991. Participation of p53 protein in the cellular response to DNA damage. *Cancer Res.* 51:6304–6311.
5. Lane, D.P. 1992. p53, guardian of the genome. *Nature.* 358: 15–16.
6. Lane, D.P. 1993. A death in the life of p53. *Nature.* 362:786–787.
7. Lotem, J., M. Peled-Kamar, Y. Groner, and L. Sachs. 1996. Cellular oxidative stress and the control of apoptosis by wild-type p53, cytotoxic compounds, and cytokines. *Proc. Natl. Acad. Sci. USA.* 93:9166–9171.
8. Polyak, K., Y. Xia, J.L. Zweier, K.W. Kinzler, and B.A. Vogelstein. 1997. A model for p53-induced apoptosis. *Nature.* 389:300–305.
9. Forrester, K., S. Ambs, S.E. Lupold, R.B. Kapust, E.A. Spillare, W.C. Weinberg, E. Felley-Bosco, X.W. Wang, D.A. Geller, E. Tzeng, et al. 1996. Nitric oxide-induced p53 accumulation and regulation of inducible nitric oxide synthase expression by wild-type p53. *Proc. Natl. Acad. Sci. USA.* 93: 2442–2447.
10. Crystal, R.G. 1991. Oxidants and respiratory tract epithelial injury: pathogenesis and strategies for therapeutic intervention. *Am. J. Med.* 91:39S–43S.
11. Denissenko, M.F., A. Pao, M. Tang, and G.P. Pfeifer. 1996. Preferential formation of benzo[a]pyrene adducts at lung cancer mutational hotspots in P53. *Science.* 274:430–432.
12. Smith, L.E., M.F. Denissenko, W.P. Bennett, H. Li, S. Amin, M. Tang, and G.P. Pfeifer. 2000. Targeting of lung cancer mutational hotspots by polycyclic aromatic hydrocarbons. *J. Natl. Cancer. Inst.* 92:803–811.
13. Rosen, A., L. Casciola-Rosen, and J. Ahearn. 1995. Novel packages of viral and self-antigens are generated during apoptosis. *J. Exp. Med.* 181:1557–1561.
14. Savill, J., A. Mooney, and J. Hughes. 1996. What role does apoptosis play in progression of renal disease? *Curr. Opin. Nephrol. Hypertens.* 5:369–374.
15. Albert, M.L., B. Sauter, and N. Bhardwaj. 1998. Dendritic cells acquire antigen from apoptotic cells and induce class I-restricted CTLs. *Nature.* 392:86–89.
16. Starcher, B.C., C. Kuhn, and J.E. Overton. 1978. Increased elastin and collagen content in the lungs of hamsters receiving an intratracheal injection of bleomycin. *Am. Rev. Respir. Dis.* 117:299–305.
17. MacMicking, J.D., C. Nathan, G. Hom, N. Chartrain, D.S. Fletcher, M. Trumbauer, K. Stevens, Q.W. Xie, K. Sokol, N. Hutchinson, et al. 1995. Altered responses to bacterial infection and endotoxic shock in mice lacking inducible nitric oxide synthase. *Cell.* 81:641–650. [published erratum at 81: 1170].
18. Nicoletti, I., G. Migliorati, M.C. Pagliacci, F. Grignani, and C. Riccardi. 1991. A rapid and simple method for measuring thymocyte apoptosis by propidium iodide staining and flow cytometry. *J. Immunol. Methods.* 139:271–279.
19. McConkey, D.J., P. Hartzell, J.F. Amador-Perez, S. Orrenius, and M. Jondal. 1989. Calcium-dependent killing of immature thymocytes by stimulation via the CD3/T cell receptor complex. *J. Immunol.* 143:1801–1806.
20. Gavrieli, Y., Y. Sherman, and S.A. Ben-Sasson. 1992. Identification of programmed cell death in situ via specific labeling of nuclear DNA fragmentation. *J. Cell Biol.* 119:493–501.
21. Hecht, S.M. 1986. DNA strand scission by activated bleomycin group antibiotics. *Fed. Proc.* 45:2784–2791.
22. Beham, A., M.C. Marin, A. Fernandez, J. Herrmann, S. Brisbay, A.M. Tari, G. Lopez-Bernstein, G. Lozano, M. Sarkiss, and T.J. McDonnell. 1997. BCL-2 inhibits p53 nuclear import following DNA damage. *Oncogene.* 15:2767–2772.
23. Lowe, S.W., E.M. Schmitt, S.W. Smith, B.A. Osborne, and T. Jacks. 1993. p53 is required for radiation-induced apoptosis in mouse thymocytes. *Nature.* 362:847–849.
24. Merritt, A.J., C.S. Potten, C.J. Kemp, J.A. Hickman, A. Balmain, D.P. Lane, and P.A. Hall. 1994. The role of p53 in spontaneous and radiation-induced apoptosis in the gastrointestinal tract of normal and p53-deficient mice. *Cancer Res.* 54:614–617.
25. Glockzin, S., A. von Knethen, M. Scheffner, and B. Brune. 1999. Activation of the cell death program by nitric oxide involves inhibition of the proteasome. *J. Biol. Chem.* 274: 19581–19586.
26. Brockhaus, F., and B. Brune. 1999. p53 accumulation in apoptotic macrophages is an energy demanding process that precedes cytochrome c release in response to nitric oxide. *Oncogene.* 18:6403–6410.

27. Hagimoto, N., K. Kuwano, Y. Nomoto, R. Kunitake, and N. Hara. 1997. Apoptosis and expression of Fas/Fas ligand mRNA in bleomycin-induced pulmonary fibrosis in mice. *Am. J. Respir. Cell Mol. Biol.* 16:91–101.
28. Lane, D. 1998. Awakening angels. *Nature.* 394:616–617.
29. Clarke, A.R., C.A. Purdie, D.J. Harrison, R.G. Morris, C.C. Bird, M.L. Hooper, and A.H. Wyllie. 1993. Thymocyte apoptosis induced by p53-dependent and independent pathways. *Nature.* 362:849–852.
30. Lowe, S.W., H.E. Ruley, T. Jacks, and D.E. Housman. 1993. p53-dependent apoptosis modulates the cytotoxicity of anticancer agents. *Cell.* 74:957–967.
31. Tamura, T., M. Ishihara, M.S. Lamphier, N. Tanaka, I. Oishi, S. Aizawa, T. Matsuyama, T.W. Mak, S. Taki, and T. Taniguchi. 1995. An IRF-1-dependent pathway of DNA damage-induced apoptosis in mitogen-activated T lymphocytes. *Nature.* 376:596–599.
32. Lassus, P., M. Ferlin, J. Piette, and U. Hibner. 1996. Anti-apoptotic activity of low levels of wild-type p53. *EMBO (Eur. Mol. Biol. Organ.) J.* 15:4566–4573.
33. Asada, M., T. Yamada, K. Fukumuro, and S. Mizutani. 1998. p21Cip1/WAF1 is important for differentiation and survival of U937 cells. *Leukemia.* 12:1944–1950.
34. Asada, M., T. Yamada, H. Ichijo, D. Delia, K. Miyazono, K. Fukumuro, and S. Mizutani. 1999. Apoptosis inhibitory activity of cytoplasmic p21(Cip-1/WAF1) in monocytic differentiation. *EMBO (Eur. Mol. Biol. Organ.) J.* 18:1223–1234.
35. Kuwano, K., R. Kunitake, M. Kawasaki, Y. Nomoto, N. Hagimoto, Y. Nakanishi, and N. Hara. 1996. p21waf-1/cip-1/sdi1 and p53 expression in association with DNA strand breaks in idiopathic pulmonary fibrosis. *Am. J. Respir. Crit. Care Med.* 154:477–483.
36. Dameron, K.M., O.V. Volpert, M.A. Tainsky, and N. Bouck. 1994. Control of angiogenesis in fibroblasts by p53 regulation of thrombospondin-1. *Science.* 265:1582–1584.
37. Savill, J., N. Hogg, Y. Ren, and C. Haslett. 1992. Thrombospondin cooperates with CD36 and the vitronectin receptor in macrophage recognition of neutrophils undergoing apoptosis. *J. Clin. Invest.* 90:1513–1522.
38. Lawler, J., M. Sunday, V. Thibert, M. Duquette, E.L. George, H. Rayburn, and R.O. Hynes. 1998. Thrombospondin-1 is required for normal murine pulmonary homeostasis and its absence causes pneumonia. *J. Clin. Invest.* 101: 982–992.
39. Okudela, K., T. Ito, H. Mitsui, H. Hayashi, N. Udaka, M. Kanisawa, and H. Kitamura. 1999. The role of p53 in bleomycin-induced DNA damage in the lung. A comparative study with the small intestine. *Am. J. Pathol.* 155:1341–1351.
40. Byrnes, R.W., J. Templin, D. Sem, S. Lyman, and D.H. Petering. 1990. Intracellular DNA strand scission and growth inhibition of Ehrlich ascites tumor cells by bleomycins. *Cancer Res.* 50:5275–5286.
41. Templin, J., L. Berry, S. Lyman, R.W. Byrnes, W.E. Antholine, and D.H. Petering. 1992. Properties of redox-inactivated bleomycins. In vitro DNA damage and inhibition of Ehrlich cell proliferation. *Biochem. Pharmacol.* 43:615–623.
42. Griffiths, S.D., A.R. Clarke, L.E. Healy, G. Ross, A.M. Ford, M.L. Hooper, A.H. Wyllie, and M. Greaves. 1997. Absence of p53 permits propagation of mutant cells following genotoxic damage. *Oncogene.* 14:523–531.
43. Corbet, S.W., A.R. Clarke, S. Gledhill, and A.H. Wyllie. 1999. P53-dependent and -independent links between DNA-damage, apoptosis and mutation frequency in ES cells. *Oncogene.* 18:1537–1544.
44. Prost, S., C.O. Bellamy, A.R. Clarke, A.H. Wyllie, and D.J. Harrison. 1998. p53-independent DNA repair and cell cycle arrest in embryonic stem cells. *FEBS Lett.* 425:499–504.
45. Chazotte-Aubert, L., P. Hainaut, and H. Ohshima. 2000. Nitric oxide nitrates tyrosine residues of tumor-suppressor p53 protein in MCF-7 cells. *Biochem. Biophys. Res. Commun.* 267:609–613.
46. MacMicking, J., Q.W. Xie, and C. Nathan. 1997. Nitric oxide and macrophage function. *Annu. Rev. Immunol.* 15:323–350.
47. Malkin, D., F.P. Li, L.C. Strong, J.F. Fraumeni, Jr., C.E. Nelson, D.H. Kim, J. Kassel, M.A. Gryka, F.Z. Bischoff, M.A. Tainsky, et al. 1990. Germ line p53 mutations in a familial syndrome of breast cancer, sarcomas, and other neoplasms. *Science.* 250:1233–1238.
48. Buhl, R., A. Meyer, and C. Vogelmeier. 1996. Oxidant-protease interaction in the lung. Prospects for antioxidant therapy. *Chest.* 110:267S–272S.
49. Baeuerle, P.A., and T. Henkel. 1994. Function and activation of NF-kB in the immune system. *Annu. Rev. Immunol.* 12: 141–179.
50. Giri, S.N., D.M. Hyde, and M.J. Schiedt. 1988. Effects of repeated administration of *N*-acetyl-L-cysteine on sulfhydryl levels of different tissues and bleomycin-induced lung fibrosis in hamsters. *J. Lab. Clin. Med.* 111:715–724.
51. McConkey, D.J. 1998. Biochemical determinants of apoptosis and necrosis. *Toxicol. Lett.* 99:157–168.
52. Hamilton, R.F., L. Li, T.B. Felder, and A. Holian. 1995. Bleomycin induces apoptosis in human alveolar macrophages. *Am. J. Physiol.* 269:L318–L325.
53. Hamilton, R.F., L.L. Iyer, and A. Holian. 1996. Asbestos induces apoptosis in human alveolar macrophages. *Am. J. Physiol.* 271:L813–L819.
54. Iyer, R., R.F. Hamilton, L. Li, and A. Holian. 1996. Silica-induced apoptosis mediated via scavenger receptor in human alveolar macrophages. *Tox. Appl. Pharmacol.* 141:84–92.
55. Bellingan, G.J., H. Caldwell, S.E. Howie, I. Dransfield, and C. Haslett. 1996. In vivo fate of the inflammatory macrophage during the resolution of inflammation: inflammatory macrophages do not die locally, but emigrate to the draining lymph nodes. *J. Immunol.* 157:2577–2585.
56. Herscowitz, H.B., R.E. Conrad, and K.J. Pennline. 1979. Alveolar macrophage-induced suppression of the immune response. *Adv. Exp. Med. Biol.* 121:459–484.
57. Savill, J., V. Fadok, P. Henson, and C. Haslett. 1993. Phagocytic recognition of cells undergoing apoptosis. *Immunol. Today.* 14:131–136.
58. Jones, H.A., J.B. Schofield, T. Krausz, A.R. Boobis, and C. Haslett. 1998. Pulmonary fibrosis correlates with duration of tissue neutrophil activation. *Am. J. Respir. Crit. Care. Med.* 158:620–628.